ELSEVIER

Journal of Molecular Catalysis A: Chemical 193 (2003) 165–176

JOURNAL OF MOLECULAR CATALYSIS A: CHEMICAL

www.elsevier.com/locate/molcata

Oxidation of phenol with H_2O_2 catalysed by Cr(III), Fe(III) or Bi(III) *N*,*N*′-bis(salicylidene)diethylenetriamine (H_2saldien) complexes encapsulated in zeolite-Y

Mannar R. Maurya [a,*], Salam J.J. Titinchi [a], Shri Chand [b]

[a] *Department of Chemistry, Indian Institute of Technology Roorkee, Roorkee 247667, India*
[b] *Department of Chemical Engineering, Indian Institute of Technology Roorkee, Roorkee 247667, India*

Received 11 March 2002; accepted 24 July 2002

Abstract

Cr(III), Fe(III) and Bi(III) complexes of *N*,*N*′-bis(salicylidene)diethylenetriamine (H_2saldien) encapsulated in zeolite-Y have been isolated and characterised by spectroscopic (IR and UV-Vis) studies and thermal as well as X-ray diffraction (XRD) patterns. Catalytic activities of these complexes for the decomposition of H_2O_2 and for the oxidation of phenol to a mixture of catechol and hydroquinone using H_2O_2 as an oxidant have been studied. A best-suited condition has been optimised by considering the concentration of substrate, reaction time, amount of catalyst, oxidant and solvent for maximum transformation of phenol. Thus, for a fixed amount of phenol (4.7 g), 0.025 g of catalyst, 5.67 g of aqueous 30% H_2O_2 and 2 ml of CH_3CN are required to carry out the reaction at 80 °C in order to have maximum phenol transformation. However, selectivity towards the formation of catechol and hydroquinone vary from catalyst to catalyst. Respective neat metal complexes have also been prepared and studied for their catalytic activities for comparing these results.

Keywords: Oxidation of phenol; Decomposition of H_2O_2; Zeolite-Y; Encapsulation; Catechol and hydroquinone formation

1. Introduction

Catalysis is known to play a key role in modern chemical technologies. Nowadays it is generally agreed that the key role in catalytic reactions is played by intermediate chemical interaction of reactive molecules with definite functional groups (active sites) of homogeneous, heterogeneous or biological (enzyme) catalysts. Modern catalytic science faces even more complicated and challenging problems. These are connected with the urgent necessity to create new highly effective industrial process, which are selective, ecologically pure and consume minimum energy. At least creating organised molecular systems, which are designed to have an optimum space arrangement, energy and orbital correspondence of the catalytic system components and substrates, can solve some of these problems.

Zeolites are one of the most important catalysts being used in chemical industries on large scale due to their inherent capabilities of product selectivity. Encapsulation of metal complexes in the super cages of zeolite matrix possess the advantages of solid heterogeneous catalysts like easy separation, ruggedness, etc., as well as share many advantageous features of homogeneous catalysts. Various transition metal complexes of H_2salen (H_2salen: *N*,*N*′-bis(salicylidene)

* Corresponding author. Fax: +91-1332-73560.
E-mail address: rkmanfcy@iitr.ernet.in (M.R. Maurya).

1381-1169/02/$ – see front matter © 2002 Elsevier Science B.V. All rights reserved.
PII: S1381-1169(02)00451-X

ethane-1,2-diamine) and its other substituted derivatives have been encapsulated in zeolite-Y matrix and their catalytic activities have been studied towards decomposition of H_2O_2 and *tert*-butyl hydroperoxide [1–3]; selective epoxidation/oxidation of olefins [4–8] and styrene [9]; oxidation of cyclohexanol and phenol [10], and selective hydrogenation [11]. Recently, oxidation of *p*-xylene using [Mn(salpn)] (H_2salpn: *N*,*N*′-bis(salicylidene)propane-1,3-diamine) encapsulated in super cages of zeolite-Y [12] and oxidation of phenol using Cr(III), Fe(III), Bi(III), Cu(II), Ni(II) and Zn(II) complexes of H_2salpn encapsulated in zeolite-Y matrix [13,14] have been reported. The *N*,*N*′-bis(salicylidene)diethylenetriamine (H_2saldien (**I**)) is potential dibasic pentadentate ligand with good flexibility and may give stable transition metal complexes. Encapsulation of these complexes in the cavity of zeolite-Y may, thus, provide better catalytic activity. In the present investigation, we have, therefore, encapsulated and characterised Cr(III), Fe(III) and Bi(III) complexes of H_2saldien (**I**) in the super cages of zeolite-Y matrix. Catalytic activities of these complexes have been studied towards the decomposition of H_2O_2 and the oxidation of phenol. Neat complexes of the above metal ions have also been prepared and their catalytic activities have been compared with the encapsulated ones. Only Mn(III) complex of H_2-5,5′-dinitrosaldien (*N*,*N*′-bis(5,5′-dinitrosalicylidene)diethylenetriamine) has been prepared and used as catalyst for the epoxidation of (*Z*)-β-methylstyrene [15].

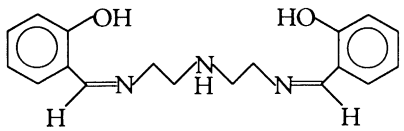

I (H_2saldien)

2. Experimental

2.1. Materials

Metal nitrates (nitrates of Cr(III), Fe(III), and Bi(III)), 30% aqueous H_2O_2 and phenol (Qualigens, India) were of Analar grade. Salicylaldehyde and diethylenetriamine (E. Merck, India) were used without further purification. All other chemicals and solvents used were also of AR grade. Zeolite-Y (Si/Al ∼ 10) was obtained from Indian Oil Corporation (R&D), Faridabad, India.

2.2. Physical methods and analysis

IR spectra were recorded as KBr pellet on a Perkin-Elmer model 1600 FT-IR spectrometer. Electronic spectra were recorded in Nujol on Shimadzu 1601 UV-Vis spectrophotometer by layering mull of sample to inside of one of the cuvette while keeping another one layered with Nujol as reference. Thermogravimetric analyses of the pure as well as encapsulated complexes were carried out using TG Stanton Redcroft STA 780. X-ray diffractograms of solid catalysts were recorded using Philips PW 1140/90 X-ray powder diffractometer with Cu Kα target at the Scientific Instrumentation Centre of our Institute. The metal contents were measured by using Perkin-Elmer model 3100 atomic absorption spectrophotometer. All catalysed reaction products were analysed using Nucon 5700 gas chromatograph fitted with FID detector, a 2 m × 2 mm (i.d.) OV-17 (s.s.) column and ORACLE 2 computer software.

2.3. Preparations

2.3.1. Preparation of ligand (H_2saldien)

H_2saldien was prepared by following the literature procedure with slight modification [16]. Salicylaldehyde (12.2 g, 0.1 mol) was dissolved in 75 ml of methanol, and to this was added a solution of diethylenetriamine (5.15 g., 0.05 mol) in 25 ml of methanol. The reaction mixture thus obtained was refluxed on a water bath for 1 h. After reducing the volume of the solvent to ca. 50 ml, the content was transferred into a beaker and excess solvent was evaporated under the current of air where viscous yellow-red oil was obtained. This was further dried in vacuum.

2.3.2. Preparation of M-Y (metal-exchanged zeolite-Y)

An amount of 5.0 g zeolite Na-Y was suspended in 300 ml distilled water containing metal nitrate (50 mmol) (nitrates of Fe(III), Cr(III) or Bi(III)). The mixture was then heated while stirring at 90 °C

for 24 h. The solid was filtered, washed with hot distilled water till the filtrate was free from any non-encapsulated metal ion content and dried for 12 h at 150 °C in air.

2.3.3. Preparation of [M(saldien)·H_2O]Cl-Y

The encapsulated complexes were prepared by general flexible ligand method [1,4]. An amount of 1.0 g M-Y and 2.5 g H_2saldien were mixed in a round bottom flask. The reaction mixture was heated at 100 °C overnight (∼14 h) in an oil bath with constant stirring. The ligand acted as solvent as well as reactant. The resulting material was taken out and extracted with methanol using Soxhlet extractor till the complex was free from unreacted H_2saldien. The non-complexed metal ions present in the zeolite were removed by exchanging with aqueous 0.01 M NaCl solution. The resulting solid was finally washed with hot distilled water till no precipitation of AgCl was observed on reacting filtrate with $AgNO_3$ solution. This was then dried at 150 °C for several hours till constant weight was achieved.

2.4. Catalytic activity studies

2.4.1. Decomposition of H_2O_2

An amount of 0.025 g of encapsulated catalyst was added to an aqueous solution of 30% H_2O_2 (5.5 g, 0.049 mol) at room temperature (25 °C) and the reaction mixture was stirred for the stipulated time (1 or 2 h). At the end of the reaction, the catalyst was filtered and the filtrate was diluted to 250 ml with distilled water. Ten millilitres of this solution was withdrawn and after addition of 20 ml of 2 M H_2SO_4 and 20 ml of distilled water, it was titrated against standard $KMnO_4$ solution. Similar experiment was also performed with neat complexes by using 0.004 g of catalyst, while keeping other conditions same as mentioned previously.

2.4.2. Oxidation of phenol

The catalytic activity measurements were carried out in a 50 ml glass reaction flask fitted with a water condenser. Phenol (4.7 g, 0.05 mol) and 30% aqueous H_2O_2 (5.67 g, 0.05 mol) were mixed in 2 ml of CH_3CN and the reaction mixture was heated with continuous stirring in an oil bath maintained at 80 °C. The catalyst for the activity test (0.025 g) was added to the reaction mixture and the reaction was considered to begin. The reaction products were analysed using a gas chromatograph after specific interval of time by withdrawing small aliquot out. The effect of various parameters such as amount of oxidant, amount of catalyst and volume of solvent have been taken into consideration in order to study their effect on the reaction. However, basic procedure is same as outlined previously.

2.4.3. Oxidation of 2,4-dichlorophenol and 1-naphthol

An amount of 2,4-dichlorophenol (8.15 g, 0.05 mol) or 1-naphthol (7.2 g, 0.05 mol) and H_2O_2 (5.67 g, 0.05 mol) was taken in 2 ml of CH_3CN and heated at 80 °C. After addition of [Cr(saldien)·H_2O]Cl-Y (0.025 g), the reaction was carried out for 4 h and at the end, the products were analysed as mentioned previously.

3. Results and discussion

3.1. Syntheses and characterisation of catalysts

Synthesis of metal encapsulated complexes in the super cages of zeolite-Y was carried out by flexible ligand method which consisted of mainly two steps: (i) the preparation of M-Y (M: Cr(III), Fe(III) and Bi(III)), which is straight forward; and (ii) the heating of metal-exchanged zeolite in excess of ligand at 100 °C for ca. 14 h. Second step allowed the insertion of the ligand in the cavity of the zeolite followed by its complexation with metal ions. Complexation of H_2saldien with Cr(III) and Fe(III) ions were accompanied by the colour change, while Bi(III) gave colourless compound. The crude mass was finally purified by Soxhlet extraction method using methanol. The remaining non-complexed metal ions in zeolite were removed by exchanging with aqueous 0.01 M NaCl solution. The percentage of metal contents estimated before and after encapsulation by atomic absorption spectroscopy (AAS) is presented in Table 1. The metal ion contents thus estimated after encapsulation are only due to the presence of metal complexes in zeolite framework. The physico-chemical properties of the metal complexes encapsulated in the zeolite-Y were confirmed by recording their IR and UV-Vis spectra, thermal analysis and X-ray powder diffraction

Table 1
Chemical composition, physical and analytical data of M-Y and encapsulated catalysts

Serial no.	Compound	Colour	Metal content (wt.%)
1	Cr-Y	Green	1.67
2	Fe-Y	Brown	0.55
3	Bi-Y	White	2.17
4	[Cr(saldien)·H_2O]Cl-Y	Light green	1.34
5	[Fe(saldien)·H_2O]Cl-Y	Light brown	0.36
6	[Bi(saldien)·H_2O]Cl-Y	White	1.90

(XRD) pattern and comparing their properties with that of the simple complexes prepared by the reaction of H_2saldien with the respective metal nitrates. The formulations of the encapsulated complexes (Table 1) are, thus, based on the respective simple complex. The Si/Al ratio of 9.67 corresponds to a unit cell of formula $Na_{18}(AlO_2)_{18}(SiO_2)_{174}$. If we consider about 250 water molecules associated with this, then, from the metal content estimated in encapsulated complexes, the calculated metal complex per unit cell corresponds to ∼1.1 for Fe-based, ∼4.2 for Cr-based and ∼1.5 for Bi-based catalysts.

3.2. TGA studies

The thermogravimetric analysis (TGA) data of the encapsulated catalysts along with the percentage weight loss at different steps and their probable assignments are presented in Table 2. All catalysts record an endothermic loss of 14–16% in the temperature range 150–280 °C due to the presence of intra-zeolite water. Though all catalysts were dried at 150 °C for several hours, it is expected that even at this temperature intra-zeolite water will remain present in the catalyst. In fact, the presence of at least four such water molecules have been reported for [Cu(salen)]-Y [10,17–19]. Thermal decomposition of remaining anhydrous moieties occurs in two steps. The exothermic loss starts immediately after the first step. This loss may be due to one water molecule and chloride ion associated with the complex. As these catalysts were treated with aqueous NaCl, the presence of Cl^- counter ion is expected in all cases. A rather small weight loss (8–10%) occurs in the next step (which starts immediately after the second step) having a wider temperature range of 275–800 °C. This is due to the decomposition of chelating ligand. A very small weight percentage loss indicates the insertion of only small amount of metal complexes in the zeolite-Y matrix.

3.3. X-ray powder diffraction studies

The X-ray powder diffraction pattern of Na-Y, its metal-exchanged zeolite M-Y (M: Cr(III), Fe(III) and Bi(III)) and encapsulated metal complexes [M(saldien)·H_2O]Cl-Y were recorded at 2θ values between 5 and 70°. Typical XRD patterns of Cr-Y and [Cr(saldien).H_2O]Cl-Y are shown in Fig. 1. All metal-exchanged and encapsulated species exhibit essentially similar pattern to that observed for Na-Y. However, slight change in the intensities of the peaks could be observed. The appearance of peaks in metal-exchanged zeolite and encapsulated ones suggest that the super cages of the zeolite are able to accommodate these complexes and the crystallinity

Table 2
Thermogravimetric analysis data of catalysts

Catalyst	Temperature range (°C)	Loss (wt.%)	Group lost[a]	Type of loss
[Cr(saldien)·H_2O]Cl-Y	150–230	16.0	nH_2O	Endothermic
	230–275	2.0	H_2O + Cl	Exothermic
	275–650	8.0	L	Exothermic
[Fe(saldien)·H_2O]Cl-Y	150–240	15.0	nH_2O	Endothermic
	240–295	4.0	H_2O + Cl	Exothermic
	295–800	10.0	L	Exothermic
[Bi(saldien)·H_2O]Cl-Y	150–280	14.0	nH_2O	Endothermic
	280–360	4.0	H_2O + Cl	Exothermic
	360–560	10.0	L	Exothermic

[a] L stands for saldien^{2-}.

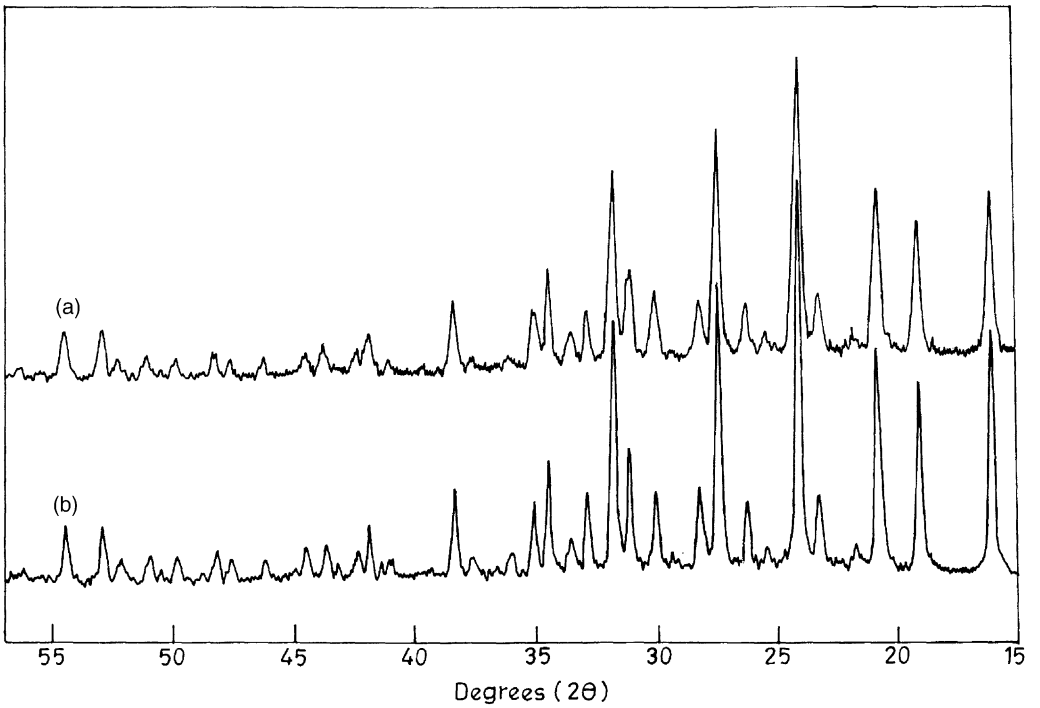

Fig. 1. XRD patterns of (a) Cr-Y, and (b) [Cr(saldien)·H_2O]Cl-Y.

of the zeolite-Y is maintained during encapsulation. Two new peaks with d values of 3.392 nm (at 2θ = 29.2) and 2.181 nm (at 2θ = 46.0) were observed in Cr-Y as well as in [Cr(saldien)·H_2O]Cl-Y. In Bi-Y as well as [Bi(saldien)·H_2O]Cl-Y, two new peaks with d values of 3.415 nm (at 2θ = 29.0) and 2.741 nm (at 2θ = 36.3) were also observed. As encapsulated complexes were carefully extracted with methanol and then re-exchanged with NaCl to remove surface species and non-complexed metal ions, respectively, the existence of new peaks in the metal-exchanged and encapsulated zeolites could be attributed to atomic level integration resulting in non-vanishing structure factor for certain peaks which were extinct in Na-Y structure. Location of any new peaks in [Fe(saldien)·H_2O]Cl-Y was not possible due to poor resolution of these peaks in the XRD pattern.

3.4. UV-Vis and IR spectral studies

Electronic absorption spectra of ligands and catalysts (encapsulated as well as neat complexes) are presented in Table 3 and the spectra of the encapsulated complexes are reproduced in Fig. 2. The spectrum of H_2saldien exhibits four bands at 402, 316, 255 and 220 nm. As molar absorptivity of the first two bands are comparatively low, these bands seem to be splitter band of n–π^* transition. Other bands are due to π–π^* and ϕ–ϕ^* transitions, respectively. A weak shoulder band also appears at 280 nm, which is assigned as intramolecular hydrogen bonding. The shoulder band is completely absent in the spectra of all complexes, thereby indicating the destruction of hydrogen bonding and coordination of phenolic oxygen to metal ion. In complexes, the first two bands merge and appear at 306–385 nm, while 255 nm band shifts to higher wave length (255–282 nm) and 220 nm band has no definite trend. The absorption spectra of encapsulated complexes are essentially similar to the corresponding neat complexes. The spectral bands appearing at 553 (weak and broad) and 385 nm (which is merging with the ligand band) in [Cr(saldien)·H_2O]Cl-Y or at 560 and 415 nm in [Cr(saldien)·H_2O]Cl compare well with the reported

Table 3
IR and electronic spectral data of ligand and its neat and encapsulated complexes

Compound	IR (cm^{-1})		λ_{max}	
	ν(C=N), (C=C)	ν(M-O)/(M-N)	Solvent	Band (nm)
H_2saldien	1583, 1634	–	MeOH	402, 316, 280, 255, 220
[Cr(saldien)·H_2O]Cl-Y	1543, 1625	412, 427, 481, 503	Nujol	553, 385, 265, 215
[Cr(saldien)·H_2O]Cl	1540, 1622	436, 480, 517	DMF	560, 415, 306, 277
[Fe(saldien)·H_2O]Cl-Y	1545, 1632	466, 499	Nujol	480, 325, 265, 230
[Fe(saldien)·H_2O]Cl	1548, 1630	466, 486	DMF	470, 308, 281
[Bi(saldien)·H_2O]Cl-Y	1542, 1636	451, 472, 506	Nujol	255, 210
[Bi(saldien)·H_2O]Cl	1542, 1620	417, 435, 463, 508	Nujol	263, 220

value for $[Cr(H_2O)_6]^{3+}$ [20], where these bands appear at 574.7 and 405 nm, respectively. Accordingly, these bands are assigned due to $^4A_{2g}(F) \rightarrow {}^4T_{2g}(F)$ (ν_1) and to $^4A_{2g}(F) \rightarrow {}^4T_{1g}(F)$ (ν_2) transitions, respectively, in an octahedral fields. The band due to $^4A_{2g}(F) \rightarrow {}^4T_{2g}(P)$ transition, which appears at 270 nm in $[Cr(H_2O)_6]^{3+}$ could not be located in present Cr(III) complexes due to strong absorption of ligand band in this region. Iron complexes exhibit one d–d band at ~480 nm as a weak band [21] while Bi(III) complexes exhibit, as expected, ligand bands only.

A partial list of IR spectral data of H_2saldien and encapsulated as well as neat complexes is also presented in Table 3. Though, IR spectra of all encapsulated complexes are essentially similar to that of neat complexes, the intensity of the peaks is weak due to low concentration of the complexes in zeolite matrix. Comparison of the band positions of ligands with metal complexes reveal the following facts: (i) the band appearing in the 2550–2700 cm^{-1} region due to intramolecular hydrogen bonding between phenolic –OH and azomethine nitrogen is absent. This observation indicates the coordination of phenolic oxygen to the metal after destruction of hydrogen bond; and (ii) the free ligand exhibits ν(C=N) (azomethine) stretch at 1583 cm^{-1}. This band shifts to lower frequency in complexes and appears at 1540–1548 cm^{-1}, indicating the involvement of azomethine nitrogen in coordination. The coordination of –NH group could not be ascertained due to the appearance of broad

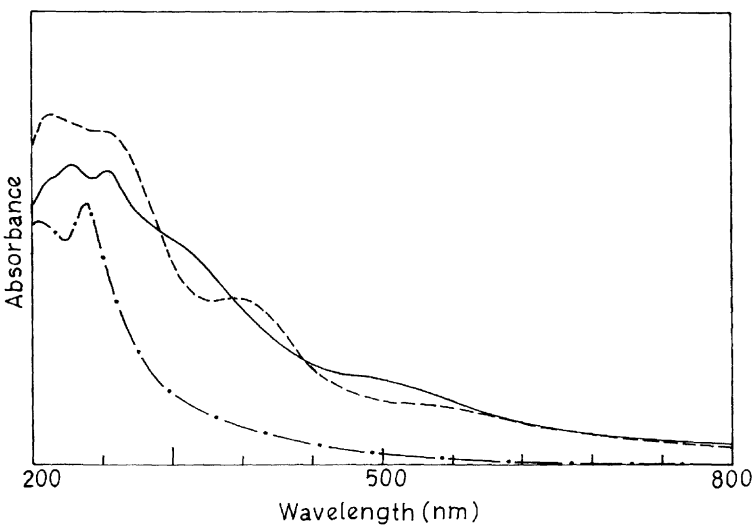

Fig. 2. Electronic spectra of: (– – –) [Cr(saldien)·H_2O]Cl-Y, (—) [Fe(saldien)·H_2O]Cl-Y, (— · —) [Bi(saldien)·H_2O]Cl-Y.

Table 4
Percentage decomposition of H_2O_2 after 1 and 2 h of contact time

Catalyst	Percentage decomposition after 1 h	TOF	Percentage decomposition after 2 h	TOF
[Fe(saldien)·H_2O]Cl-Y	4.9	44.9	6.2	24.4
[Cr(saldien)·H_2O]Cl-Y	11.0	95.7	12.6	39.9
[Bi(saldien)·H_2O]Cl-Y	13.3	174.5	15.9	74.2
[Fe(saldien)·H_2O]Cl	3.5	164.5	5.9	137.5
[Cr(saldien)·H_2O]Cl	1.8	74.8	7.0	148.3
[Bi(saldien)·H_2O]Cl	4.7	313.0	11.8	389.4

Turn over frequency (TOF): moles of substrate converted per mole of metal (in solid catalyst) per hour.

band of water ~3400 cm^{-1}. However, appearance of two to four bands in the low frequency region (400–550 cm^{-1}) should indicate the coordination of phenolic oxygen, azomethine nitrogen and nitrogen of –NH group. Thus, IR data further supports the encapsulation of the complex in the zeolite matrix.

3.5. Decomposition of H_2O_2

The catalytic activity of all encapsulated complexes for the decomposition of H_2O_2 at different reaction times was tested and the relevant data are presented in Table 4. The decomposition of H_2O_2 catalysed by Fe-based catalyst after 1 h reaction time is rather slow (4.9%), while Cr- and Bi-based catalysts showed decomposition of 11.0 and 13.3%, respectively. Increasing contact time to 2 h has improved partially the decomposition and were found in the order: Bi(III) (15.9%) > Cr(III) (12.6%) > Fe(III) (6.2%). The turn over frequency (TOF) calculated for the decomposition of H_2O_2 after 1 and 2 h of contact time is presented in Table 4. The TOF for 1 h of contact follows the same order as for percentage decomposition. Due to marginal increase in percentage decomposition of H_2O_2 in the next 1 h, there is considerable decrease in TOF during that period. However, the order with respect to the catalysts is same as noted previously.

The catalytic activity of neat complexes in the decomposition of H_2O_2 at two different reaction times (e.g. 1 and 2 h) has also been determined and the data are is presented in Table 4. It is clear from the TOF values that neat complexes show better catalytic activity than the encapsulated ones. It is expected as number of metal centres in 0.004 g of neat catalysts are higher than the encapsulated one where only 0.025 g of catalysts are used.

3.6. Oxidation of phenol

The catalytic oxidation of phenol usually gives two products catechol and hydroquinone as shown by Eq. (1). These products are the only expected ones, as –OH group of phenol is *ortho* and *para* directing. Similar oxidation using H_2O_2 as an oxidant were also conducted with three different catalysts, viz. [Cr(saldien)·H_2O]Cl-Y, [Fe(saldien)·H_2O]Cl-Y and [Bi(saldien)·H_2O]Cl-Y in CH_3CN. Only two products, i.e. catechol and hydroquinone were obtained with a mass balance of about 96% for all catalysts. Minor product (e.g. polymeric materials), if any, is not detectable in GC under the condition used herein. For comparison, their respective neat metal complexes, viz. [Cr(saldien)·H_2O]Cl, [Fe(saldien)·H_2O]Cl and [Bi(saldien)·H_2O]Cl have also been examined for their catalytic activities. In order to find suitable reaction conditions to get maximum oxidised products for a fixed amount of phenol, effect of various parameters, such as, amount of catalyst, H_2O_2 concentration (moles of H_2O_2 per mole of phenol) and volume of solvent have been taken into consideration.

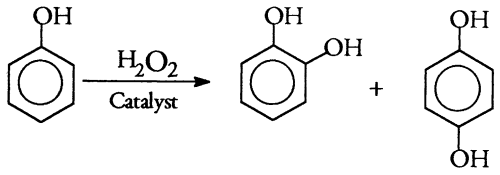

(1)

Using three different concentrations of aqueous 30% H_2O_2, viz. 0.015 mol (1.7 g), 0.03 mol (3.4 g)

and 0.05 mol (5.67 g) for a fixed amount of phenol (4.7 g) and catalyst [Cr(saldien)·H_2O]Cl-Y (0.025 g), the percentage of phenol conversions are 15.3, 31.2 and 45.0%, respectively. For these concentrations of H_2O_2, the percent selectivity for the conversion of H_2O_2 follows the order: 50.3% (0.015 mol) < 53.0% (0.03 mol) < 45.0% (0.05 mol). These results suggest that oxidation of phenol is highest with 1:1 phenol/H_2O_2 molar ratio, though selectivity of H_2O_2 conversion is relatively low at this ratio. Further increment in H_2O_2 concentration hardly improved the conversion. This clearly suggests that large concentration of oxidant is not an essential condition to maximise phenol transformation. Similarly, out of three different weights of 0.01, 0.025 and 0.03 g of catalyst, an amount of 0.025 g for all three catalysts was found to be sufficient enough for the effective phenol conversion. Variation in the volume of the solvent was also studied by taking 1, 2 and 4 ml of CH_3CN. It was observed that for 4.7 g of phenol, 0.025 g of catalyst and 5.67 g of 30% H_2O_2, 2 ml of CH_3CN was sufficient enough to carry out the reaction to get good transformation of phenol. Thus, all conditions as concluded previously were considered essential and applied for the maximum transformation of phenol into a mixture of catechol and hydroquinone. In order to compare the efficiency of the catalysts under best-required conditions, the percentage of phenol conversion and the percentage of the formation of catechol and hydroquinone were plotted as a function of time and are presented in Figs. 3–5.

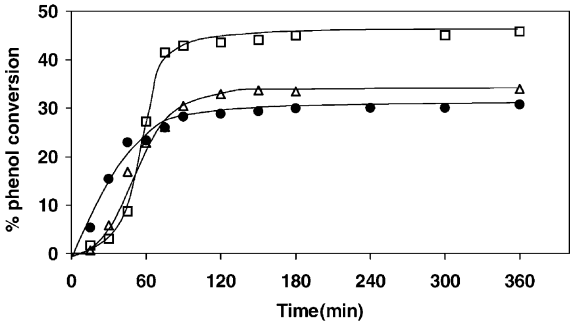

Fig. 3. Phenol oxidation: (□) [Cr(saldien)·H_2O]Cl-Y, (●) [Fe(saldien)·H_2O]Cl-Y, (△) [Bi(saldien)·H_2O]Cl-Y.

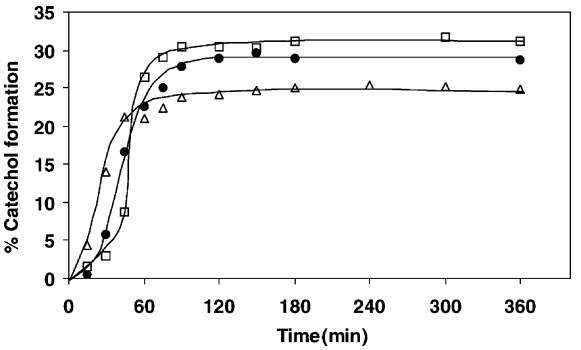

Fig. 4. Percentage catechol formation: (□) [Cr(saldien)·H_2O]Cl-Y, (●) [Fe(saldien)·H_2O]Cl-Y, (△) [Bi(saldien)·H_2O]Cl-Y.

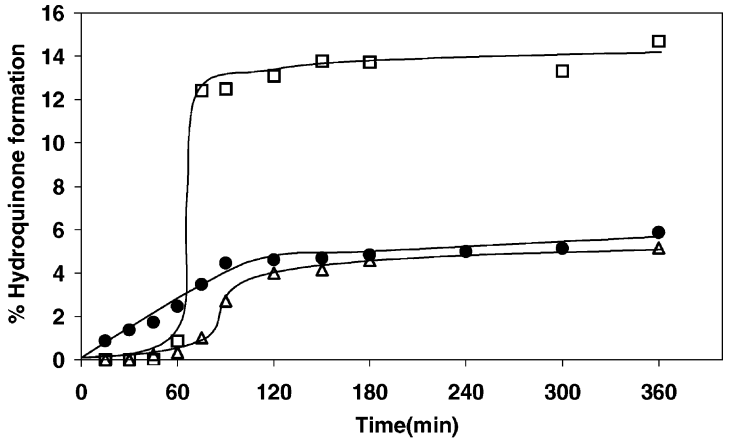

Fig. 5. Percentage hydroquinone formation: (□) [Cr(saldien)·H_2O]Cl-Y, (●) [Fe(saldien)·H_2O]Cl-Y, (△) [Bi(saldien)·H_2O]Cl-Y.

The plot presented in Fig. 3 shows that phenol conversion increases considerably in the first 75 min for Cr-based catalyst and reaches to a steady state thereafter. The activities of Fe- and Bi-based catalyst were fast enough till first 60 and 90 min, respectively, and slowly go down in the next 30 min in both cases. Among these three catalysts, [Cr(saldien)·H_2O]Cl-Y performed best and gave a highest conversion of about 45%, whereas, [Bi(saldien)·H_2O]Cl-Y and [Fe(saldien)·H_2O]Cl-Y recorded conversions of about 33 and 28%, respectively.

Fig. 4 presents percentage catechol formation as a function of reaction time. A maximum of 31% of catechol formation was recorded with Cr-based catalyst. On the other hand, using Bi-based catalyst, catechol formation was only about 28%, which was followed by Fe-based catalyst (24%). In comparison to catechol formation, the hydroquinone formation (Fig. 5) is much lower in all the cases and follow the order: [Cr(saldien)·H_2O]Cl-Y (13%) > [Fe(saldien)·H_2O]Cl-Y (5%) > [Bi(saldien)·H_2O]Cl-Y (4%). Increasing the reaction time from 6 to 24 h does not show appreciable change in either phenol transformation or catechol and hydroquinone formation. Fig. 6 summarises all these results together as bar diagram after 6 h of reaction time. On comparing plots it is clear that [Cr(saldien)·H_2O]Cl-Y is much better catalyst in comparison to [Bi(saldien)·H_2O]Cl-Y, which in turn is better than [Fe(saldien)·H_2O]Cl-Y in terms of phenol transformation as well as formation of catechol and hydroquinone. However, in terms of selectivity, the later two catalysts are more selective (∼84%) for the catechol formation, while less selective (∼16%) for the hydroquinone formation (Table 5). The [Cr(saldien)·H_2O]Cl-Y has shown only ∼69% selectivity for the formation of catechol and ∼31% for the formation of hydroquinone.

Table 5
Selectivity of catechol and hydroquinone formation after 6 h of reaction time

Catalyst	Catechol (%)	Hydroquinone (%)
[Cr(saldien)·H_2O]Cl-Y	68.8	31.2
[Fe(saldien)·H_2O]Cl-Y	83.9	16.1
[Bi(saldien)·H_2O]Cl-Y	84.8	15.2
[Cr(saldien)·H_2O]Cl	63.9	36.1
[Fe(saldien)·H_2O]Cl	63.8	36.2
[Bi(saldien)·H_2O]Cl	70.5	29.5

Catalytic oxidation of phenol using the corresponding neat complexes, viz. [Cr(saldien)·H_2O]Cl, [Fe(saldien)·H_2O]Cl and [Bi(saldien)·H_2O]Cl as catalyst and H_2O_2 as oxidant have also been studied in CH_3CN. A similar trend, i.e. higher conversion of phenol with 0.05 moles of H_2O_2, as noted previously was also observed among the three concentrations of oxidant, viz. 0.015, 0.03 and 0.05 moles for a fixed amount of phenol (4.7 g) and catalyst (0.004 g). However, conversion was considerably lower in comparison to that of encapsulated ones and followed the order: [Cr(saldien)·H_2O]Cl (31%) > [Fe(saldien)·H_2O]Cl (22%) > [Bi(saldien)·H_2O]Cl (21%) after 6 h of reaction time. The Fig. 7 plotted for the phenol conversion as a function of time indicates that conversion also increases in the first 60 min considerably and reaches the steady state in next few min. The percentage catechol and hydroquinone

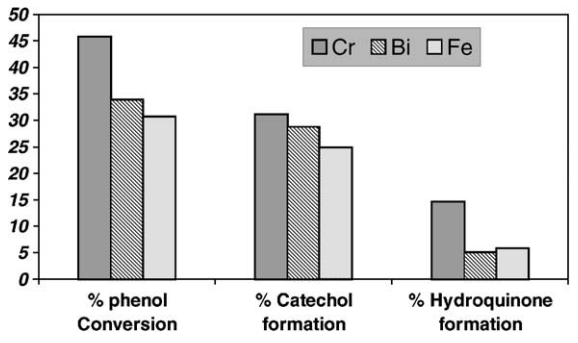

Fig. 6. Bar diagram showing phenol conversion and catechol and hydroquinone formation for various catalysts (encapsulated). Inset shows notation for respective catalyst.

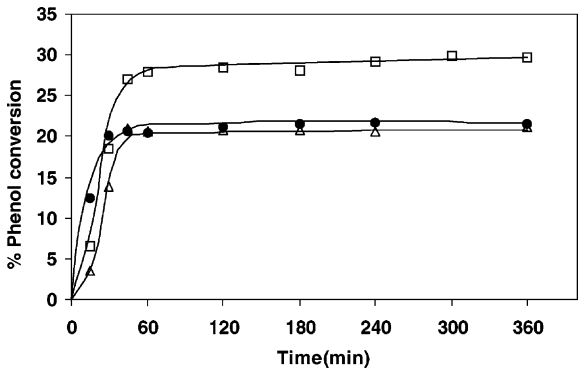

Fig. 7. Phenol oxidation: (□) [Cr(saldien)·H_2O]Cl, (●) [Fe(saldien)·H_2O]Cl, (△) [Bi(saldien)·H_2O]Cl.

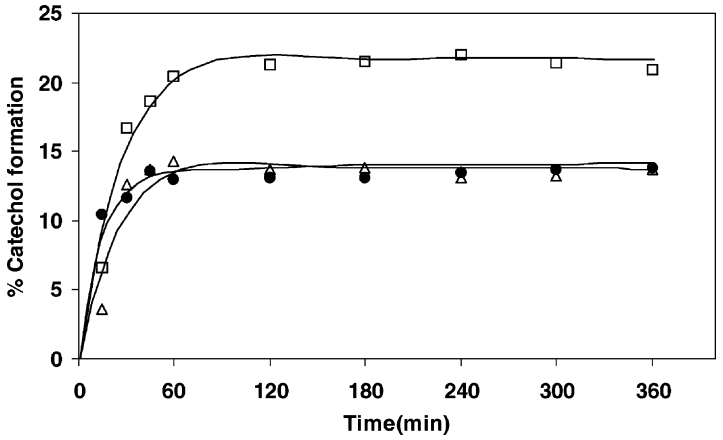

Fig. 8. Percentage catechol formation: (□) [Cr(saldien)·H_2O]Cl, (●) [Fe(saldien)·H_2O]Cl, (△) [Bi(saldien)·H_2O]Cl.

formations versus time profiles are shown in Figs. 8 and 9 and reveal that the catechol formation is always higher than hydroquinone formation. However, within the catechol formation the order: Cr (22%) > Fe (16%) = Bi (16%) while hydroquinone is nearly same and is about 8.0 ± 0.5% in all cases after 6 h of reaction time.

3.7. Catalytic activities comparison of neat and encapsulated complexes

On comparing the data for neat complexes and complexes encapsulated in zeolite matrix, it is clear that encapsulated complexes are always better over non-encapsulated ones for the transformation of phenol. Following factors may be responsible for this. (i) The neat complexes may lead to the formation of μ-oxo dimer or possibility of the dimerisation as such during reaction, which is responsible for the lower catalytic performance. Dimerisation of [Cu(5-X-salen)] (where X: H, CH_3O) during re-crystallisation has also been observed [22]. (ii) Neat complexes being active in the first cycle are partially destroyed during the prolonged contact time while no such possibility exists in encapsulated complexes. However, selectivity of these catalysts towards the product formation differs with the increment of phenol conversion. The selectivity to percentage catechol formation versus percentage conversion of phenol profiles for all catalysts during 6 h reaction time are shown in Fig. 10. This indicates that selectivity of catechol formation is relatively better with encapsulated complexes. However, with the conversion of phenol it slowly goes down with time and follow the order: Bi(III) (86%) > Fe(III) (84%) > Cr(III) (72%). In neat complexes selectivity of formation of catechol suddenly decreases from ∼98 to 62% at 20% conversion of phenol with Fe(III) and Bi(III) complexes, while from 92 to 71% at about 30% conversion with Cr(III) complex. Thus, it can be concluded that at the expense of phenol conversion selectivity of the formation of catechol decreases while selectivity of hydroquinone increases. However, either conversion of phenol or formation of a mixture of catechol and hydroquinone are all stabilised after about 6 h of reaction time and no more change in their formations are observed beyond this time.

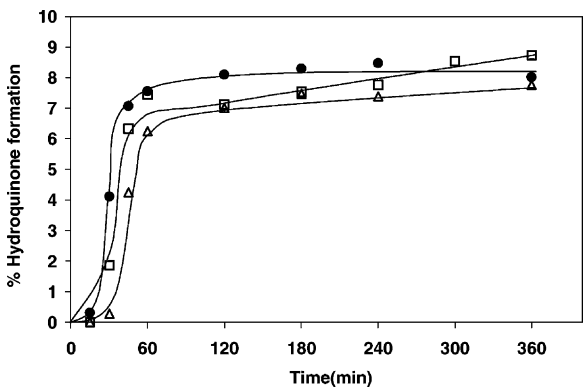

Fig. 9. Percentage hydroquinone formation: (□) [Cr(saldien)·H_2O]Cl, (●) [Fe(saldien)·H_2O]Cl, (△) [Bi(saldien)·H_2O]Cl.

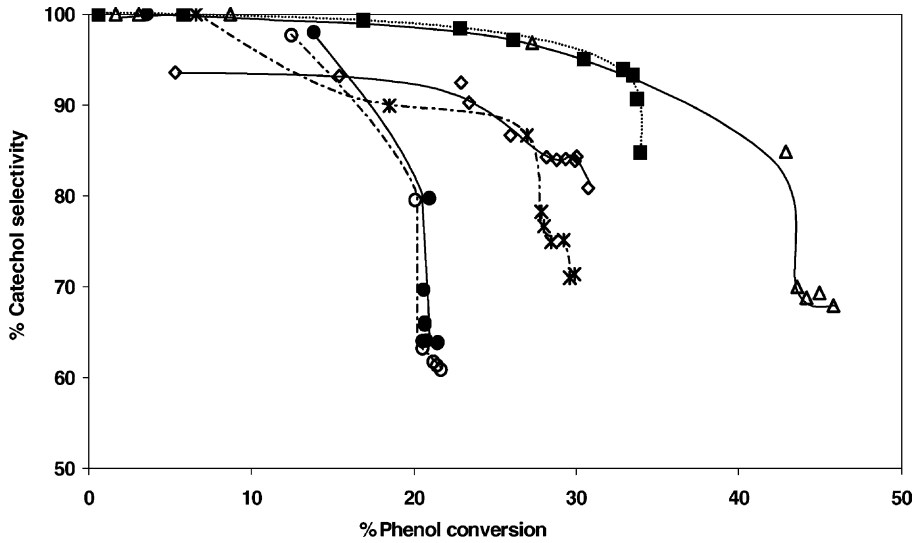

Fig. 10. Selectivity to percentage catechol formation vs. percentage phenol conversion: (△) [Cr(saldien)·H_2O]Cl-Y, (■) [Bi(saldien)·H_2O]Cl-Y, (◇) [Fe(saldien)·H_2O]Cl-Y, (✱) [Cr(saldien)·H_2O]Cl, (●) [Bi(saldien)·H_2O]Cl, (○) [Fe(saldien)·H_2O]Cl.

3.8. Oxidation of 2,4-dichlorophenol and 1-naphthol

Using the typical reaction conditions optimised for the oxidation of phenol, oxidation of 2,4-dichlorophenol and 1-naphthol was also carried out. As we go from smaller to bulkier substrates, their entrance through the opening of the zeolite pore becomes more and more difficult and would result in lower catalytic activity. As expected, only about 4% conversion of 2,4-dichlorophenol was observed due to branching of phenol. However, oxidation of 1-naphthol was found to be about 11%. Although, we expect better conversion for 2,4-dichlorophenol than 1-naphthol due to relatively smaller size of the former, the two deactivating groups (i.e. chloro substituents) are probably responsible for less conversion.

4. Summary and conclusions

The integrity of metal complexes encapsulated in the cavities of zeolite-Y was confirmed by spectroscopic studies as well as chemical and thermal analysis. This was further supported by the fact that no leaching of metal ion was detected in the solution when a blank reaction was carried out (5.5 g H_2O_2 and 0.025 g catalyst in 2 ml CH_3CN at 80 °C). Besides, the lower percentage conversion for the oxidation of 2,4-dichlorophenol or 1-naphthol using H_2O_2 as an oxidant further supports the encapsulation of metal complexes in the super cages of the zeolite-Y matrix. Steric hindrance would make their entrance difficult through channels of the zeolite to reach the proximity of the catalyst and thus responsible for its poor performance.

It is concluded from the catalytic data that the encapsulated complexes are better catalysts than neat ones. Under best-suited reaction conditions, catechol formation is always higher than hydroquinone formation. However, at the expense of phenol conversion selectivity of the formation of catechol decreases, while selectivity of hydroquinone increases in the beginning, but their formation stabilise after ∼6 h of reaction time. Comparable IR spectral patterns of fresh and used encapsulated catalysts suggest that these can be used further for catalytic study.

Acknowledgements

S.J.J.T. thanks Indian Council for Cultural Relation (ICCR) for fellowship. The authors are thankful to

Prof. S. Ray of Metallurgical and Materials Engineering Department, IIT Roorkee, for a fruitful discussion.

References

[1] C.R. Jacob, S.P. Varkey, P. Ratnasamy, Microporous Mesoporous Mater. 22 (1998) 465.
[2] C.R. Jacob, S.P. Varkey, P. Ratnasamy, Appl. Catal. A: Gen. 168 (1998) 353.
[3] S. Deshpande, D. Srinivas, P. Ratnasamy, J. Catal. 188 (1999) 261.
[4] C. Bowers, P.K. Dutta, J. Catal. 122 (1990) 271.
[5] P.-P. Knops-Gerrits, D.D. Vos, F. Thibaut-Starzk, P.A. Jacobs, Nature 369 (1994) 543.
[6] D.D. Agrawal, R.P. Bhatnagar, R. Jain, S. Srivastava, J. Chem. Soc., Perkin. Trans. 2 (1990) 989.
[7] M.J. Sabater, A. Corma, A. Domenech, V. Fornés, H. Garcia, Chem. Commun. (1997) 1285.
[8] S. Koner, Chem. Commun. (1998) 593.
[9] S.P. Varkey, C.R. Jacob, Indian J. Chem. 37A (1998) 407.
[10] C. Ratnasamy, A. Murugkar, S. Padhye, S.A. Pardhy, Indian J. Chem. 35A (1996) 1.
[11] S. Kowalak, R.C. Weiss, K.J. Balkus, J. Chem. Soc., Chem. Commun. (1991) 57.
[12] C.R. Jacob, S.P. Varkey, P. Ratnasamy, Appl. Catal. A: Gen. 182 (1999) 91.
[13] M.R. Maurya, S.J.J. Titinchi, S. Chand, I.M. Mishra, J. Mol. Catal. A: Chem. 180 (2002) 201.
[14] M.R. Maurya, S.J.J. Titinchi, S. Chand, Appl. Catal. A: Gen. 228 (2002) 177.
[15] K. Srinivasan, P. Michaud, J.K. Kochi, J. Am. Chem. Soc. 108 (1986) 2309.
[16] W.M. Coleman, R.K. Boggess, J.W. Hughes, L.T. Taylor, Inorg. Chem. 20 (1981) 700.
[17] G. Meyer, D. Wöhrle, M. Mohl, G. Schulz-Ekloff, Zeolites 4 (1984) 30.
[18] H. Diegruber, P.J. Plath, G. Schulz-Ekloff, J. Mol. Catal. 24 (1984) 115.
[19] G. Schulz-Ekloff, D. Wöhrle, V. Iliev, E. Ignatzek, A. Andreev, Stud. Surf. Sci. Catal. 46 (1989) 315.3.
[20] F.A. Cotton, G. Wilkinson, Advance Inorganic Chemistry, 3rd ed., Wiley, New Delhi, 1993, p. 838.
[21] G. Wilkinson, R.D. Gillard, J.A. McCleverty (Eds.), Comprehensive Coordination Chemistry, vol. 1, Pergamon Press, Oxford, 1987, p. 253.
[22] M.M. Bhadbhade, D. Srinivas, Inorg. Chem. 32 (1993) 5458.